ELSEVIER

International Journal of Thermal Sciences 41 (2002) 891–898

International Journal of Thermal Sciences

www.elsevier.com/locate/ijts

Absorption of water vapour in the falling film of water–lithium bromide inside a vertical tube at air-cooling thermal conditions

Marc Medrano, Mahmoud Bourouis, Alberto Coronas *

Centre d'Innovació Tecnològica en Revalorització Energètica i Refrigeració (CREVER), Universitat Rovira i Virgili, Autovia de Salou, s/n, 43006, Tarragona, Spain

Received 26 June 2001; accepted 12 November 2001

Abstract

In the absorbers of air-cooled water–lithium bromide absorption chillers, the absorption process usually takes place inside vertical tubes with external fins. In this paper we have carried out an experimental study of the absorption of water vapour over a wavy laminar falling film of water–lithium bromide on the inner wall of a smooth vertical tube. The control variables for the experimental study were; absorber pressure, solution mass flow rate, solution concentration and cooling water temperature. Relatively high cooling water temperatures were selected to simulate air-cooling thermal conditions. The parameters considered to assess the performance of the absorber were; the mass absorption flux, the outlet solution degree of subcooling and the falling film heat transfer coefficient. The results indicate that in water cooling thermal conditions the mass absorption fluxes are in the range 0.001–0.0015 $kg{\cdot}m^{-2}{\cdot}s^{-1}$, whereas in air-cooling thermal conditions the range of mass absorption values decreases to 0.00030–0.00075 $kg{\cdot}m^{-2}{\cdot}s^{-1}$.

Keywords: Absorption; Falling film; Air-cooling; Air-cooled absorber

1. Introduction

The water–lithium bromide (LiBr) absorption systems which are used mainly in large cooling capacity applications (industry, large buildings, etc.) require water from cooling towers to reject heat. However, the middle and low capacity residential and commercial systems are dominated by the more compact air-cooled compression systems. Absorption machines should be air-cooled in order to become competitive at lower capacities.

In the last decade, many Japanese and Korean manufacturers of absorption machines jointly with Gas companies have taken up projects to develop air-cooled double effect air conditioning prototypes with water–lithium bromide [1–3]. The main problem for the development of these air-cooled machines is the large heat exchange surface required, which implies more expensive and larger equipment. Moreover, to be able to dissipate heat to air, the working conditions in absorber and condenser are shifted to higher temperatures and concentrations, thereby increasing the risk of crystallisation. Theoretically [4,5], no crystallisation occurs when a single effect absorption machine is operated at 45 °C in the absorber and the condenser, if the evaporator temperature is kept above 10 °C.

Most of the experimental studies on falling film absorption process over vertical tubes with water–LiBr solution [6–13] were carried out with the falling film on the outer surface of smooth tubes, and also with absorption heat dissipation by means of cooling water at relatively low temperatures in the range 20–35 °C. Only Kurosawa et al. [14] experimentally studied the falling film absorption process inside smooth and rough vertical tubes. They performed the experiments at a solution concentration of 55% and a cooling water temperature in the range 19–32 °C, and found falling film heat transfer coefficients in the range 0.4–2.0 $kW{\cdot}m^{-2}{\cdot}K^{-1}$.

Under the framework of a national project, we have carried out the design of an air-cooled absorber to be incorporated in a water chiller prototype. The absorber consists of vertical finned tubes with the falling film and the water vapour flowing concurrently inside the tubes. The aim of the first phase of the project is to study the absorption process inside a single water-cooled vertical tube absorber at air-cooling thermal conditions. The objective

* Correspondence and reprints.
E-mail address: crever@crever.urv.es (A. Coronas).

1290-0729/02/$ – see front matter
PII: S1290-0729(02)01383-2

Nomenclature

A	heat transfer area	m^2	
C_p	specific heat	$kJ \cdot kg^{-1} \cdot K^{-1}$	
D	diameter	m	
g	gravitational acceleration	$m \cdot s^{-2}$	
h	convective heat transfer coefficient	$kW \cdot m^{-2} \cdot K^{-1}$	
j	mass absorption flux	$kg \cdot m^{-2} \cdot s^{-1}$	
H	specific enthalpy	$kJ \cdot kg^{-1}$	
m	mass flow rate	$kg \cdot s^{-1}$	
Nu	Nusselt number $= \frac{h_s \delta}{\lambda}$		
P	pressure	kPa	
Q	heat rate	kW	
Re	Reynolds number $= \frac{4\Gamma}{\mu} = \frac{4\delta \cdot v\rho}{\mu}$		
T	temperature	°C	
U	overall heat transfer coefficient	$kW \cdot m^{-2} \cdot K^{-1}$	
X	concentration (weight % LiBr)		

Greek symbols

δ	film thickness $= \left(\frac{3\mu\Gamma}{\rho^2 g}\right)^{1/3}$	
Γ	$= m/\pi D_i$, mass flow rate per unit of wetted perimeter	$kg \cdot m^{-1} \cdot s^{-1}$
λ	thermal conductivity	$kW \cdot m^{-1} \cdot K^{-1}$
μ	dynamic viscosity	$N \cdot s \cdot m^{-2}$
ν	kinematic viscosity	$m^2 \cdot s^{-1}$
ρ	density	$kg \cdot m^{-3}$

Subscripts

Abs	absorber
ae	cooling water
e	external
eq	equilibrium
HE	heat exchanger
i	internal
in	inlet
M	mass
out	outlet
p	wall
Rot	flowmeter
s	solution
SUB	subcooling
v	vapour phase

of this paper is to present the experimental results and the relevant conclusions.

2. Description of experimental set-up

The main components of the experimental set-up shown in Fig. 1 are the absorber, the generator, the LiBr solution loop, the cooling water loop, and control and measurement devices. The system is designed to operate in a continuous mode.

The absorber consists of: two stainless steel concentric tubes of 1.5 m length, the liquid and vapour distributors at the top, and a weak solution collector at the bottom. The inner absorber tube has an inside diameter of 22.1 mm and a polished inner wall surface. Over this surface the falling film solution and the water vapour from the generator flow down concurrently. Cooling water flows countercurrently in the annular space between the concentric tubes removing the heat of absorption. The weak solution leaving the absorber is collected in a small receiver at the bottom before returning to the generator.

To distribute the solution entering the absorber, a plastic cylindrical filter located concentrically to the absorber is used. The water vapour from the generator enters the absorber through a ring distributor. At the top and the bottom of the absorber, two concentric peepholes are mounted to check the proper wetting of the falling film. Fig. 2 shows a schematic of the top of the absorber, which illustrates the arrangement of the upper peephole, and the liquid and vapour distributors.

The generator consists of a stainless steel cylindrical tank with a capacity of about 15 l. Three electrical heaters with an overall power of 4.0 kW are arranged at the bottom of the generator. The working pressure of the system is controlled indirectly by means of the temperature control of the solution in the generator.

The LiBr solution loop consists of a magnetic coupling gear pump (P1) with a variable speed controller, a precision flowmeter (R1), a water cooled heat exchanger cooler (HE1) and a heater tank (HT3). The pump moves the solution from the bottom to the top of the absorber at a height of about 3 meters. The strong solution leaving the pump is cooled down with tap water in the heat exchanger (HE1) and is heated up in the electric heater (HT3) to the set inlet temperature before entering the absorber.

The cooling water loop consists of a 0.140 m^3 capacity water tank, a centrifugal pump (P2), a flowmeter (F2), the absorber jacket, and a heat exchanger (HE2). This heat exchanger (HE2) cools the hot water leaving the absorber below the absorber inlet temperature so that it can be controlled by the 4.0 kW heating system provided in the water tank.

The experimental set-up has two auxiliary tanks. The auxiliary tank (TA1) is used to drain the generator in case of operation problems. The other auxiliary tank (TA2) is used to collect and weigh the condensed water that is separated when the working concentration of strong solution is increased.

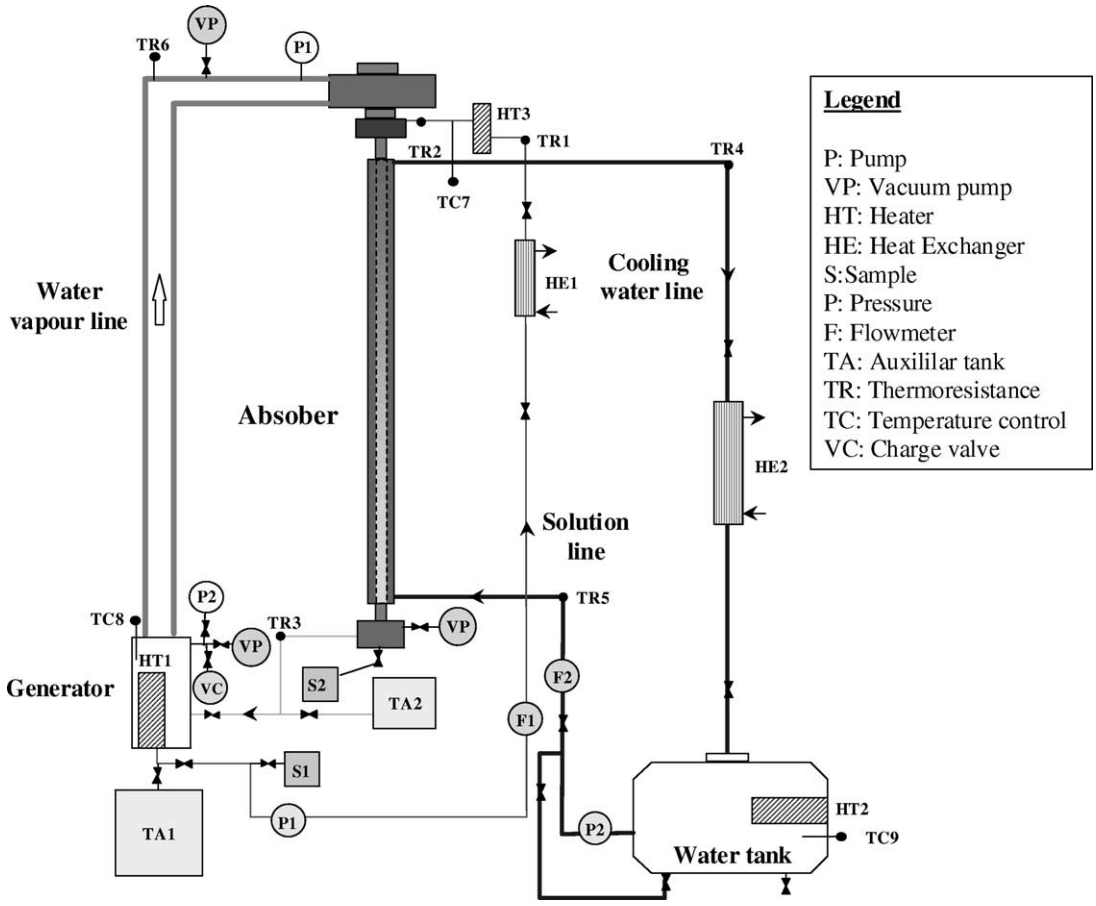

Fig. 1. Schematic diagram of the experimental set-up.

The purge system to remove non-absorbable gases consists of a liquid ring vacuum pump and a liquid nitrogen cold trap. The system was able to be operated at an acceptable leak rate below 2×10^{-8} kPa·m^3·s^{-1}.

The inlet and outlet solutions can be sampled in two pre-evacuated flasks (S1 and S2). The concentration of inlet and outlet solutions are determined by a precision Anton Paar densimeter, applying the water–LiBr density correlation as a function of temperature and concentration [15].

To perform the experiments, the readily available commercial water–LiBr solution that is typically used in the absorption water chillers was used. This solution contains lithium molibdate (Li_2MoO_4) as corrosion inhibitor and does not have additives for heat and mass transfer enhancement. The concentration of this commercial solution was accurately measured and was found to be 54.8% by weight of LiBr.

3. Experimental measurements

Table 1 shows the measured experimental variables and the accuracy of the corresponding measurement instruments.

3.1. Test conditions

The variables considered for the parametric study of the absorber performance are the cooling water temperature, the absorber pressure, the solution flow rate and the inlet solution concentration. The temperature of the strong solution entering the absorber was kept between 5 and 10 °C above the inlet cooling water temperature. The nominal working conditions and the investigated ranges are summarised in Table 2.

3.2. Performance parameters

The following parameters are selected to assess the absorber performance; the absorber thermal load, the mass absorption flux, the outlet degree of subcooling and the falling film heat transfer coefficient. The thermophysical properties were taken from our property database, which contains the most up-dated literature correlations with the widest validity ranges [5].

The *absorber thermal load* is defined as the heat released in the absorber which is removed by the cooling water and is calculated as:

$$Q_{\mathrm{Abs}} = m_{\mathrm{ae}} Cp_{\mathrm{ae}} (T_{\mathrm{ae,out}} - T_{\mathrm{ae,in}}) \quad (1)$$

Table 1
Measured variables and accuracy of the corresponding instruments

Measured variable	Instrument	Accuracy
Volumetric flow rate of strong solution before entering the absorber, $m_{s,in}$	Flowmeter	$\pm 1.0 \times 10^{-6}$ m^3·s^{-1}
Volumetric flow rate of cooling water, m_{ae}	Flowmeter	$\pm 1.4 \times 10^{-5}$ m^3·s^{-1}
Temperature of weak solution leaving the absorber, $T_{s,out}$	Pt100 probe	±0.025 °C
Temperature of strong solution entering the absorber, $T_{s,in}$	Pt100 probe	±0.025 °C
Absorber pressure, P_{Abs}	Piozoresistive pressure transducer	±0.035 kPa
Temperature of inlet cooling water, $T_{ae,in}$	Pt100 probe	±0.025 °C
Temperature of outlet cooling water, $T_{ae,out}$	Pt100 probe	±0.025 °C
Temperature of solution leaving the cooler HE1, T_{HE1}	Pt100 probe	±0.025 °C
Temperature of water vapour, T_v	Pt100 probe	±0.5 °C
Concentration of strong solution entering the absorber, $X_{s,in}$	Anton Paar densimeter	±0.1% weight
Concentration of weak solution leaving the absorber, $X_{s,out}$	Anton Paar densimeter	±0.1% weight

Table 2
Nominal conditions and working range of the experimental study

	Nominal	Range
Temperature of cooling water, $T_{ae,in}$	35 °C	30–40 °C
Reynolds number of cooling water, Re_{ae}	6000	6000
Absorber pressure, P_{Abs}	1.3 kPa[a]	1.0–2.2 kPa
Reynolds number of solution, Re	∼ 150	50–300
Concentration of inlet solution, $X_{s,in}$	57.9 mass% LiBr	57.9–60.0 mass% LiBr

[a] This absorber pressure corresponds to the evaporator temperature of 11 °C.

The *mass absorption flux* is the absorbed mass flow rate per unit mass transfer surface and is calculated by matching the heat fluxes in solution and water sides. The solution side absorber load is expressed by:

$$Q_{Abs} = m_{s,in}H_{s,in}(T_{s,in}, X_{s,in}) - m_{s,out}H_{s,out}(T_{s,out}, X_{s,out}) + j \cdot A_M H_v(T_v, P_{Abs}) \quad (2)$$

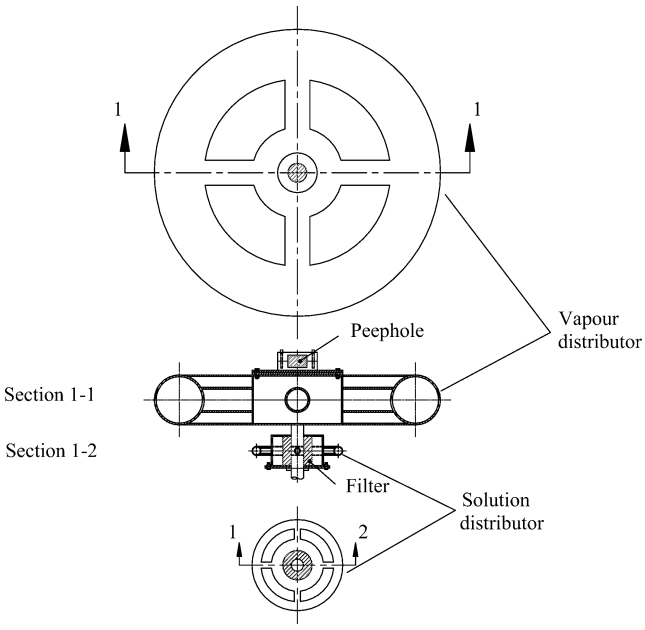

Fig. 2. Details of the solution and vapour distributors at the top of the absorber.

The above equation was solved numerically, taking into account the overall and partial mass balances of the solution in the absorber.

The *degree of subcooling* of the solution leaving the absorber is the deviation of the actual outlet solution temperature from the equilibrium solution temperature at the absorber pressure and the outlet solution concentration. High subcooling values indicate that the solution could have absorbed more refrigerant and is an indication of the ineffectiveness of absorber.

$$\Delta T_{SUB} = T_{eq,out} - T_{s,out} \quad (3)$$

The *falling film heat transfer coefficient* is given by:

$$h_s = \left[\frac{1}{U} - \frac{D_e}{2\lambda_p}\ln\frac{D_e}{D_i} - \frac{D_e}{D_i}\frac{1}{h_{ae}}\right]^{-1} \quad (4)$$

A relatively high heat transfer coefficient (∼ 8.5 kW·m^{-2}·K^{-1}) on the cooling water side was maintained by working at a Reynolds number of 6000. As the heat transfer resistance on water side was rather low (2–10% of total resistance), the uncertainty in the evaluation of the falling film coefficient was reduced.

The overall heat transfer coefficient is given by:

$$U = \frac{Q_{Abs}}{A\Delta T} \quad (5)$$

The driving potential for heat transfer independent of the outlet conditions is chosen:

$$\Delta T = T_{eq,in} - T_{ae,in} \quad (6)$$

An uncertainty analysis of the obtained experimental absorber parameters was carried out. The average relative

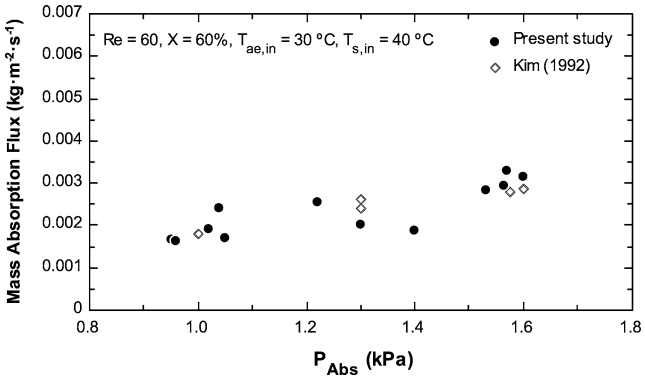

Fig. 3. Comparison of the mass absorption flux with the experimental data of Kim [6].

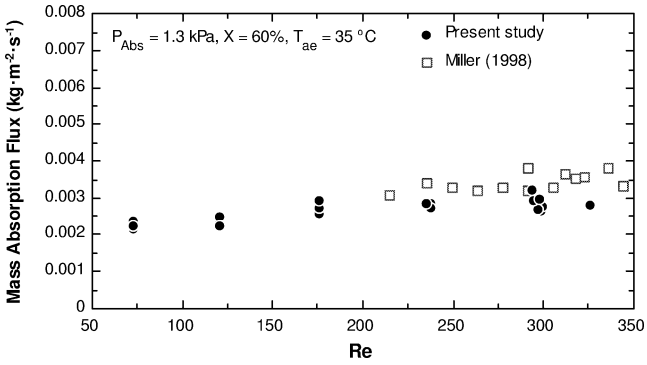

Fig. 4. Comparison of mass absorption flux with the experimental data of Miller [12].

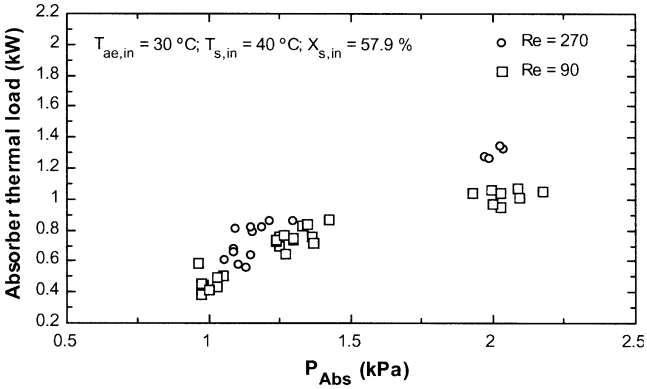

Fig. 5. Effect of absorber pressure on absorber thermal load.

error of the thermal absorber load, mass absorption flux, falling film heat transfer coefficient, degree of subcooling was around 7%, 15%, 9% and 3%, respectively.

4. Results

In this section, some preliminary tests for falling film visualisation, comparison results with published data and a parametric study of the absorber performance in the typical range of working conditions are presented.

4.1. Visualisation of the falling film

It was ensured that the plastic filter gave an uniform distribution of the solution at the absorber inlet, creating a falling film that completely wetted the inner wall. Wetting tests were also carried out, starting with high flow rates which was reduced at constant intervals until the film broke down. The film break-down was observed at a Reynolds number of about 40. Morioka and Kiyota [16] found that Reynolds number greater than 25 were required to keep the outer surface of vertical glass tube fully wetted. The agreement between both experimental studies is quite good, especially considering that the critical Reynolds number can have a large variation depending on the treatment and roughness of the surface.

4.2. Comparison with published literature data

The experimental data of two studies [6,12] on the absorption of water vapour by a falling film outside vertical tubes were compared with the present results at the same inlet conditions. As the mass absorption flux is normalised to the mass transfer surface, which allows us to compare with different absorber geometries, it was selected as the parameter for comparison.

Fig. 3 compares present results with those of Kim [6]. The agreement between the data of both experimental studies is very good, with a maximum deviation being lower than the 11% at an absorber pressure of 1.6 kPa.

Fig. 4 gives the comparison of the experimental results of Miller [12] with present results for the mass absorption flux versus the Reynolds number. The experimental data of both studies shows again a good agreement, with a maximum deviation below 25%.

The above comparisons show that no significant differences in mass absorption flux are observed between the inner wall case (present study) and the outer wall case [6,12].

4.3. Sensitivity study

A sensitivity analysis of the performance parameters of the absorber was carried out.

4.3.1. Effect of absorber pressure

The driving force for mass transfer through the vapour–liquid interface can be expressed as the difference between the partial pressure of water–vapour in vapour phase (which is equal to total pressure if non-absorbable gases are negligible) and the vapour pressure of water–LiBr solution at a given temperature and concentration. Thus, the higher is the absorber pressure, the greater is the potential for vapour transfer to the falling film.

Fig. 5 shows that the absorber load increases as the absorber pressure increases, at an inlet solution concentration of 57.9% wt. At 1.0 kPa of absorber pressure and at a low

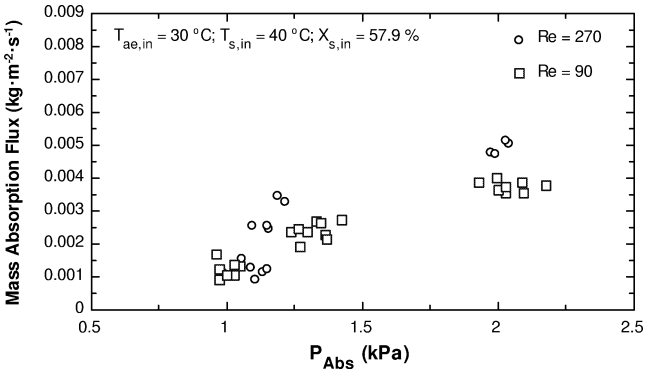

Fig. 6. Effect of absorber pressure on mass absorption flux.

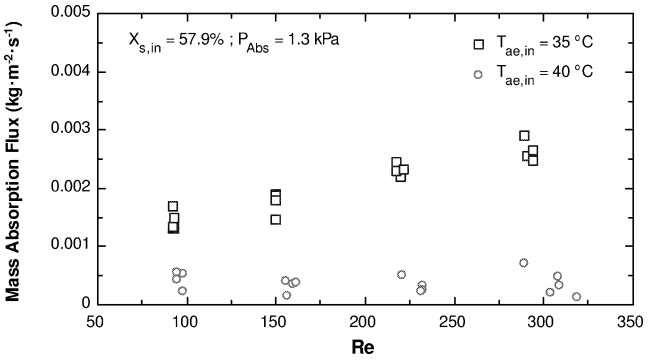

Fig. 7. Effect of solution mass flow rate on mass absorption flux.

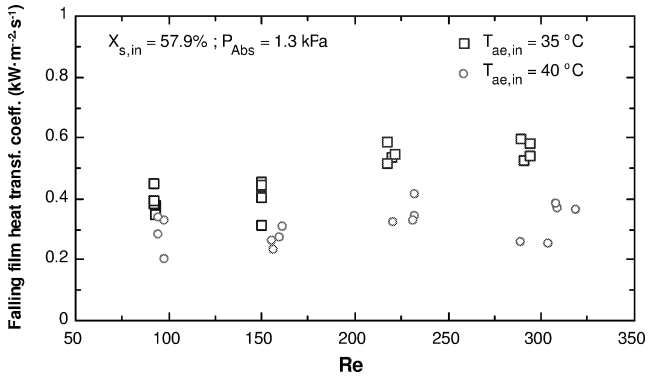

Fig. 8. Effect of solution flow rate in falling film heat transfer coefficient.

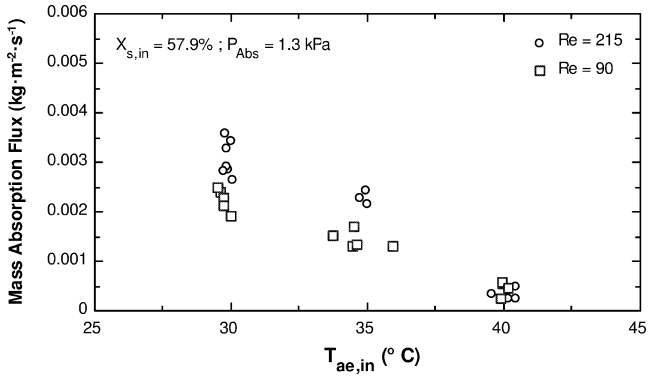

Fig. 9. Effect of cooling water temperature on mass absorption flux.

flow rate (Reynolds number of 90), the load is only of 0.4 kW, whereas it reaches to about 1.0 kW when the absorber pressure is set at 2.1 kPa.

Results in Fig. 6 show the influence of the absorber pressure on the mass absorption flux. The mass flux has a 5-fold increase when absorber pressure is increased from 1.0 kPa to 2.1 kPa, at a constant Reynolds number of 270. This significant increase in absorption mass flux is caused by the increase of the driving potential. The observed range of mass fluxes at typical water cooling conditions (absorber pressure 1.0 kPa, cooling water temperature of 30 °C and solution concentration of 57.9% wt.) is 0.001–0.0015 $kg \cdot m^{-2} \cdot s^{-1}$.

In the following sensitivity studies, the absorber pressure has been set to 1.3 kPa, which corresponds to an evaporator temperature of about 11 °C. These values simulate typical conditions for an air-cooled water–LiBr absorption machine.

4.3.2. Effect of solution flow rate

The influence of the solution mass flow rate on absorber performance was evaluated at a solution concentration of 57.9% wt. and at four different flow rates of about 80, 60, 42 and 26 $kg \cdot h^{-1}$, which correspond to Reynolds numbers of 290, 220, 150 and 100. All these Reynolds numbers fall within the wavy-laminar regime of falling film ($25 < Re < 1000$), which mostly prevails in the commercial absorption machines.

Fig. 7 shows how the Reynolds number affects the mass absorption flux at two cooling water temperatures. At a cooling water temperature of 35 °C, the mass flow rate increases with Reynolds number. A mass absorption flux increase of about 85% is observed from a Reynolds number change of 100 to 300. When the cooling water temperature is set at 40 °C, the potential for mass transfer is reduced and the mass absorption flux falls to a nearly constant value of 0.0005 $kg \cdot m^{-2} \cdot s^{-1}$.

Fig. 8 represents the falling film heat transfer coefficient versus the solution mass flow rate at the cooling water temperatures of 35 and 40 °C. The heat transfer coefficient shows a similar trend to the absorption flux, i.e., increasing with Reynolds number. The observed range of heat transfer coefficients is 0.2–0.6 $kW \cdot m^{-2} \cdot K^{-1}$.

4.3.3. Effect of cooling water temperature

Similar to the observed trends of other experimental studies on falling film absorbers [6,17], the mass absorption flux decreases almost linearly with increasing cooling water temperature. The lower heat transfer rate increases the bulk solution temperature, which implies a rise in the solution vapour pressure. The resulting reduction in the mass transfer driving force decreases the mass absorption flux, as seen in Fig. 9. At a cooling water temperature of 30 °C and a Reynolds number of 90, the mass flow rate is about 0.0025 $kg \cdot m^{-2} \cdot s^{-1}$, whereas it is only 0.0005 $kg \cdot m^{-2} \cdot s^{-1}$ when the cooling water temperature is 40 °C at the same Reynolds number.

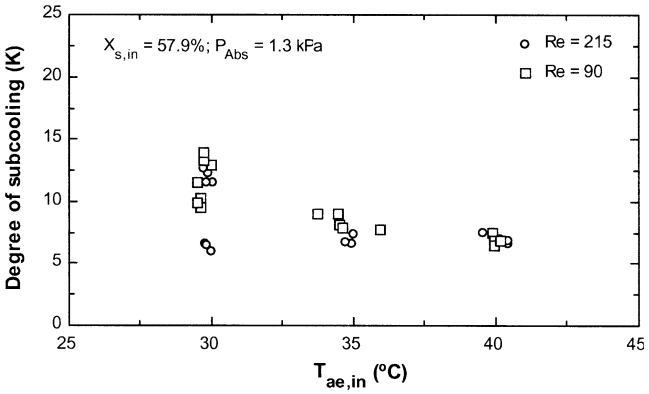

Fig. 10. Effect of cooling water temperature on subcooling of outlet solution.

Fig. 10 shows the influence of cooling water temperature on the degree of subcooling of outlet solution. Subcooling is slightly reduced when cooling water temperature is increased and it is not affected by the solution flow rate. At lower temperature driving forces, the absorber operates more effectively. Although the amount of absorbed vapour is lower, it is not far away from the highest theoretical amount that could be absorbed if saturation conditions were reached. The high degrees of subcooling (8–14 °C) indicate that the lower part of the absorber is working essentially as a heat exchanger.

From the above discussion, it can be deduced that when the temperature of cooling water is increased to simulate air-cooling conditions, the heat and mass transfer driving forces are so low that the absorption process is nearly stopped at the studied concentration levels. As the cooling air temperature and the absorber pressure are set by external conditions, the LiBr solution at absorber inlet should be concentrated in order to increase the driving potential and to enhance the absorption process. In the next section the effect of changing the solution concentration from 57.9% to 60.0% by weight of LiBr is analysed.

4.3.4. Effect of solution concentration

As the concentration of LiBr in solution increases, the vapour pressure of solution decreases and the mass transfer driving force increases. Thus, at typical thermal conditions of air-cooled absorbers, an apparently simple way to keep the same mass driving force as in cooling water conditions is to work with a more concentrated solution. Nevertheless, the solubility limit of the LiBr in water restricts practical operation to concentrations above 64% wt. However, the absorber operation at higher concentrations without crystallisation is possible by adding other lithium-based salts that increase the solubility range of the mixture.

Fig. 11 illustrates how the solution inlet concentration affects the mass absorption flux at a cooling water temperature of 40 °C and at the studied range of Reynolds numbers. As expected, the mass absorption flux increases when the concentration of the solution entering the absorber is increased. At a Reynolds number of 100, the mass absorption flux has

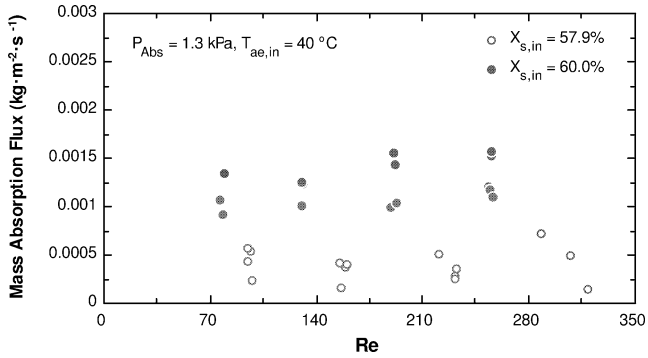

Fig. 11. Effect of solution concentration on mass absorption flux.

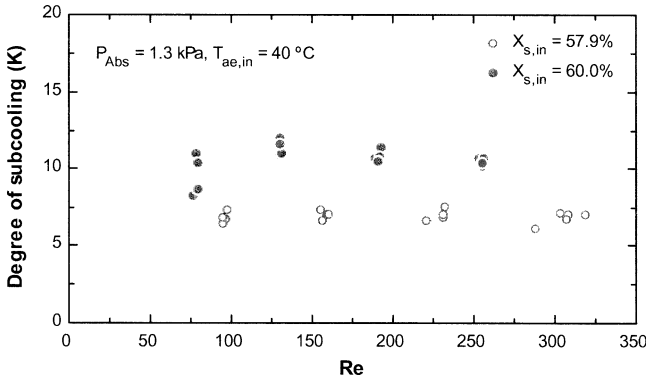

Fig. 12. Effect of solution concentration on subcooling of outlet solution.

an increase of about 100% for a 2% change in solution concentration from 57.9% to 60.0%.

Fig. 12 presents the variation of the degree of subcooling at absorber outlet with Reynolds number. At a Reynolds number of 100, the subcooling increases by about 4 °C when solution concentration is increased from 57.9 to 60.0% wt. The observed trend of subcooling shows again that when the driving potential for mass transfer increases, more water vapour is absorbed, but the absorber operates less effectively.

5. Conclusions

Experiments on the falling film absorption of aqueous solution of lithium bromide inside a vertical tube were carried out at water and air-cooling thermal conditions. The main conclusions of this study are:

- No significant differences in mass absorption flux were observed between the results of this study for inner wall falling film and those for the outer wall by other investigators.
- The relatively high degrees of subcooling (8–14 °C) indicate that the lower part of the absorber acts basically as a heat exchanger. Thus, shorter tubes are recommended to reduce subcooling.
- At typical conditions of water cooled absorbers (absorber pressure of 1.0 kPa, cooling water temperature

of 30 °C and inlet solution concentration of 57.9% wt.) the mass absorption fluxes are in the range 0.001–0.0015 $kg \cdot m^{-2} \cdot s^{-1}$, whereas in typical air-cooling conditions (absorber pressure of 1.3 kPa, water temperature of 40 °C, solution concentration of 60.0% wt.) the mass flux range decreases to 0.00030–0.00075 $kg \cdot m^{-2} \cdot s^{-1}$.

- To increase the heat and mass transfer driving force, higher salt concentrations are required. However, practical operation with water–lithium bromide restricts the maximum salt concentration to about 64% due to the crystallisation limit. The absorber operation at higher concentrations without crystallisation is possible by adding other lithium based salts that increase the solubility range of the mixture.

Acknowledgements

This work was done within the scope of the Spanish Programme for Technical Research (PROFIT). M. Medrano would like to thank CIRIT for a fellowship.

References

[1] Y. Yoshida, R. Kawakami, H. Kawaguchi, K. Ooka, O. Ooishi, Development of an air-cooled absorption packaged air conditioning unit, in: Internat. Gas Research Conference, 1995 November 6–9, Cannes, France, Vol. IV, pp. 106–115.

[2] S. Tongu, Y. Makino, Practical operating of small-sized air-cooled double-effect absorption chiller-heater by using lithium bromide and aqueous, in: Internat. Absorption Heat Pump Conference, 1994 January 19–21, New Orleans, Lousiana, AES, Vol. 31, ASME, 1993, pp. 125–132.

[3] T. Okano, Y. Asawa, M. Fujimoto, N. Nishiyama, Y. Sanai, Development of an air-cooled absorption refrigerating machine using a new working fluid, in: Internat. Absorption Heat Pump Conference, 1994 January 19–21, New Orleans, Lousiana, AES, Vol. 31, ASME, 1993, pp. 311–314.

[4] J.M. Landauro-Paredes, F.A. Watson, F.A. Holland, Experimental study of the operating characteristics of a water–lithium bromide absorption cooler, Chem. Engrg. Res. Des. 61 (1983) 362–370.

[5] M. Medrano, Desarrollo de un absorbedor tubular vertical enfriado por aire para un climatizador de absorción de agua–bromuro de litio (development of an air-cooled vertical tube absorber for an absorption air conditioner using water–lithium bromide), Ph.D. Thesis, Universitat Rovira i Virgili, Tarragona, Spain, 2001.

[6] K.J. Kim, Performance evaluations of LiCl and LiBr for absorber design applications in the open cycle absorption refrigeration system, in: Internat. Absorption Heat Pump Conference, 1996 September 17–20, Montreal, Canada, Vol. II, pp. 769–778.

[7] K.J. Kim, N.S. Berman, S.C. Chaud, B.D. Wood, Absorption of water vapour into falling films of aqueous lithium bromide, Internat. J. Refrig. 18 (1995) 486–494.

[8] K.J. Kim, S. Kulankara, K.E. Herold, C. Miller, Heat transfer additives for use in high temperature applications, in: Internat. Absorption Heat Pump Conference, 1996 September 17–20, Montreal, Canada, Vol. I, pp. 89–97.

[9] I. Morioka, M. Kiyota, R. Nakao, Absorption of water vapor into a film of aqueous solution of libr falling along a vertical pipe, JSME Internat. J. Ser. B 36 (2) (1993) 351–356.

[10] A. Beutler, L. Hoffmann, G. Alefeld, K. Gommed, K. Grossmann, A. Shavit, Experimental investigations of heat and mass transfer in film absorption on horizontal and vertical tubes, in: Internat. Absorption Heat Pump Conference, 1996 September 17–20, Montreal, Canada, Vol. I, pp. 409–419.

[11] D.S. Sheehan, P. Prescott, H. Perez-Blanco, Investigation of additive effectiveness with infrared sensor dynamic surface tension measurements, in: Internat. Absorption Heat Pump Conference, 1996 September 17–20, Montreal, Canada, Vol. I, pp. 75–82.

[12] W.A. Miller, M. Keyhani, The correlation of simultaneous heat and mass transfer experimental data for aqueous lithium bromide vertical falling film absorption, J. Solar Energy Engrg. Trans. ASME 123 (1) (2001) 30–42.

[13] S. Kulankara, Effect of enhancement additives on the absorption of water vapor by aqueous lithium bromide, Ph.D. Thesis, University of Maryland, College Park, 1999.

[14] S. Kurosawa, Y. Nagaoka, A. Yoshida, O. Masato, Y. Kunugi, Development of air-cooled gas-fired absorption water chiller-heater, in: Working Fluids and Transport Phenomena in Advanced Absorption Heat Pumps (Annex 14), Vol. 2, IEA Heat Pump Center, 1990, pp. 9, 41, 42.

[15] R.J. Lee, R.M. Di Guilio, S.M. Jeter, A.S. Teja, Properties of lithium bromide–water solutions at high temperatures and concentrations—II: density and viscosity, ASHRAE Trans. 96 (1) (1990) 709–728.

[16] I. Morioka, M. Kiyota, Absorption of water vapor into a lithium bromide water solution film falling along a vertical plate, Trans. Japan Soc. Mech. Engrg. Ser. B 53 (485) (1987) 236–240.

[17] M. Vallés, Estudio experimental del proceso de absorción de fluidos orgánicos con intercambiadores de placas (experimental study of the absorption process of organic fluids with plate heat exchanger, Ph.D. Thesis, Universitat Rovira i Virgili, Tarragona, Spain, 2000.